Determination of Optical Constants N and K for MgO Nanopowder Using Kramers-Kronig Equation

Misagh Ghamari[*], Mahdi Ghasemifard, Ehsan Fathi

Nano Technology Laboratory, Engineering department, Esfarayen University of technology, Esfarayen, Iran,98195-96619

Abstract- **Nano MgO was synthesized using auto combustion method(ACM). The XRD results confirm the existence of periclase as a main phase. In order to measure the particle size, TEM images were used and histogram of particle size from TEM showed the size in the range of 30-80nm. The results of Uv-vis spectroscopy show the band gap of 4.11 ev for nano magnesium oxide. From FTIR some optical constants such as refractive index, extinction coefficient, real and imaginary part of dielectric and loss function were obtained using kramers-kronig equation.**

Keywords- kramers-kronig; optical properties; refractive index; FTIR.

I. INTRODUCTION

Nano materials are good candidates for many applications in science and industry due to some extraordinary features and brilliant properties. Magnesium oxide with high melting point, catalytic properties[1-3], pollutant absorbents[4], gas sensor[5], nanocomposite for dental cements[6], environmental remediation[7] and other features is one of the most valuable material in this field. Since this material is inexpensive and non poisonous[8], its application is going to be more interesting nowadays. Insulating metal oxides have attracted wide interest in recent years due to their potential applications as support for metal nano-particles in electronic devices, heterogeneous catalysts and gas sensing systems. MgO is especially promising candidate to its wide bandgap and the good chemical, thermal stability and optical properties[9, 10] . The compound is easy to prepare due to the high oxygen affinity and low melting temperature of Mg. Therefore a lot of researches has been carried out to synthesis and characterization of nano magnesium oxide either as powder[11-30] or thin film[5, 31-37]. In this study using combustion method[27, 38] nano MgO is prepared and then optical constants is identified with kramres-kronig equation.

II. EXPERIMENTAL PROCEDURE

Magnesium nitrate(molar mass $148.3 \frac{g}{mol}$), citric and nitric acid and ammonium hydroxide are starting materials. After dissolving magnesium nitrate in dionized water, a mixture of citric and nitric acid was added to the base solution. after adjusting temperature and pH, reflux was done for 12h in order to increase the homogenity of solution. In the next step sol was transferred into gel by heating and finally the gel was burned using nitric acid as fuel. As prepared obtained material then was put into the furnace and white powder of nano magnesium oxide was produced at 800°c. In order to characterize the properties of nano MgO, some tests including TEM, XRD, Uv-vis and FTIR were conducted on sample.

III. RESULTS AND DISCUSION

A. XRD results

XRD can be used to identify the phase analysis of materials. In this work X-ray with $1.54A^{0}$ wavelength and nickel as filter have been used. Fig.1 shows the XRD of nano MgO in the range of 0-110 degree. According to Fig.1 periclase as main phase is detectable. Lattice parameter of nano MgO is $4.2112A^{0}$.
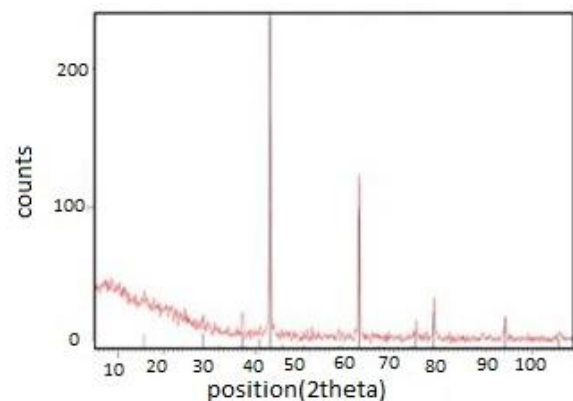

Fig.1. XRD of nano MgO calcined at 800°c.

From Schrrer equation crystallite size can be calculated [39]as follow:

$$D_{XRD} = \frac{0.9\lambda}{FWHH \cdot \cos\theta} \qquad (1)$$

Where D is crystallite size, λ is wavelength, FWHH broadening of the maximum peak at half intensity as radian and θ is Bragg angle as degree. Crystallite size and main Bragg angles of XRD were listed in table1.

TableI. crystallite size and mail Bragg angles obtained from XRD for nano MgO.

No	h	k	l	d(A)	2theta(deg)	I %	Crystallite size(nm)
1	1	1	1	2.43163	36.937	4.0	8.37
2	2	0	0	2.10564	42.917	100.0	8.53
3	2	2	0	1.48905	62.304	39.0	7.73
4	3	1	1	1.26982	74.691	5.0	8.32
5	2	2	2	1.21578	78.630	10.0	9.3
6	4	0	0	1.05281	94.052	8.0	8.96
7	3	3	1	0.96621	105.734	2.0	5.26

Other information about crystal structure have been shown in table2. Lattice parameter of cubic structure is 4.21A^o that is in good agreement with others.

TableII. crystallographic features of nano MgO from XRD.

No	Crystallographic feature	quantity
1	Crystal system	Cubic
2	Space group	Fm3m
3	Space group number	225
4	a (Å)	4.2112
5	b (Å)	4.2112
6	c (Å)	4.2112
7	Alpha (°)	90.0000
8	Beta (°)	90.0000
9	Gamma (°)	90.0000
10	Measured density	3.56
11	Volume of cell	74.68
[38]	a (Å)	4.21

B. TEM investigations

TEM image of nano magnesium oxide is shown in Fig.2. It is evident from Fig.2 that particle size of nano magnesia is in the range of 30-80nm. The shape of particles are nearly spherical to cubic and non-agglomerated as reported before[9, 40].
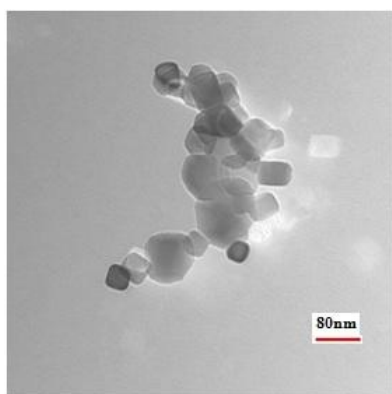

Fig.2. TEM of nano magnesium oxide.

Fig.3 shows particle size distribution of nano MgO according to TEM. As can be observed the peak is located at around 50nm.
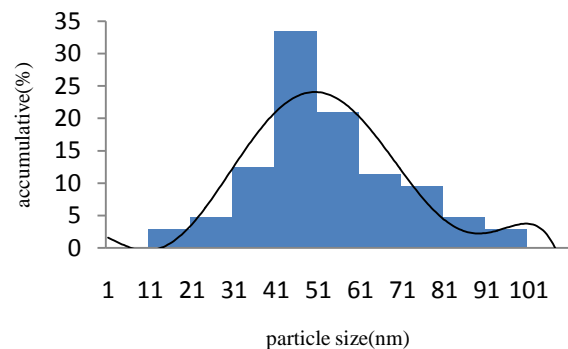

Fig.3. size distribution of nano MgO associated with TEM.

C. UV-vis spectroscopy

Because of nanostructure and discernible particle size distribution of nano MgO, the optical properties of these materials are investigated in great detail. Fig.4 shows Uv-vis spectroscopy of nano magnesia in 200-900nm.
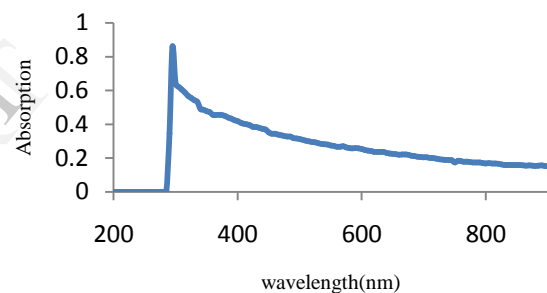

Fig.4. Uv-vis spectroscopy of nano magnesium oxide in 200-900nm

As can be seen from Fig.4 absorption edge of sample is 285nm that means all of the wavelengths smaller than 285nm absorbed by nano MgO and others can pass through the material. A strong absorption in Uv region and sharp slop can imply this phenomena. This absorption on 285nm can attribute to transactions of electrons on orbital structures. Electronic structure of Mg is $3s^2$ and for oxygen is $2p^4$. According to this, energy absorbed in this region is associated with charge transfer from magnesium to oxygen ligand as $M \rightarrow L$.

From Uv-vis there is also possibility to calculate band gap. The absorption coefficient (α), should be evaluated from the optical transmittance data using the Lambert's principle[41], $\alpha = -\frac{1}{t}\ln(T)$, where T is the transmittance and t is the diameter of nano-particles which measured in TEM. The absorption coefficient as a function of photon energy can be expressed from well-known relation as[42], $(\alpha h\nu)^n = C\left(\frac{hc}{\lambda} - E_g\right)$, where C is a constant, (α) absorption coefficient, (hc/λ) the incident photon energy and E_g is optical band gap energy. By plotting $(\alpha h\nu)^2$ versus (hc/λ), E_g can be evaluated from the extrapolated linear portion of the plot. The value of $(\alpha h\nu)^2$ as a function of photon energy is shown in Fig 5. The band gap associated

with plotting $(\alpha h v)^2$ versus (hc/λ) is 4.11ev that is different from others[43].
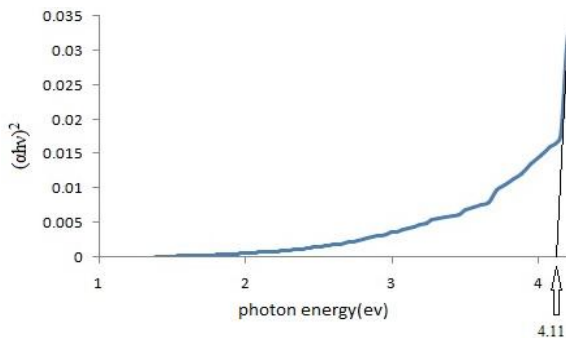

Fig.5. Absorption coefficient $(\alpha h v)^n$ versus photon energy for nano MgO.

D. FTIR calculations

The optical characterization gives valuable information about the structural parameters of the powder. Using Fourier Transform Infrared spectroscopy (FTIR) and Kramers-Kronig (K-K) analysis the optical constants of nano magnesium oxide evaluated as a function of wavenumber (ω) [44]. FTIR spectrum of the nano-MgO recorded in KBr pellet is shown in Fig.6. The presence of hydroxyl groups (OH stretching band) appeared at around 3446cm^{-1}. No characteristic band of nitrate ions at 1464 cm^{-1} is observed from the FTIR spectra indicating the complete decomposition of Mg precursor during the heat treating process. In the FTIR spectrum of the MgO powder calcined at 800 °C, the absorption bands of NO$_3$-group at 616 and 619 cm^{-1} disappear because of the complete decomposition of nitrate. The absorption peak at 1122 cm^{-1} is also observed from the spectra showing the C-O absorption. It is well-known that H$_2$O and CO$_2$ molecules are easily chemisorbed onto nano MgO surface when exposed to the atmosphere. As reported before, the broad vibration band at 3440–3450 cm^{-1} is associated with the OH stretching vibrations of water molecules, while those at 1630–1640 cm^{-1} are associated with their bending mode[45]. The absorption band at 862 cm^{-1} is contributed to the characteristic absorption peak of cubic MgO. It can be seen that the intense characteristic vibration of cubic MgO exists in the band ranging from 500-1000 cm^{-1} with the absorption peak at 862 cm^{-1} indicating the complete formation of cubic MgO.
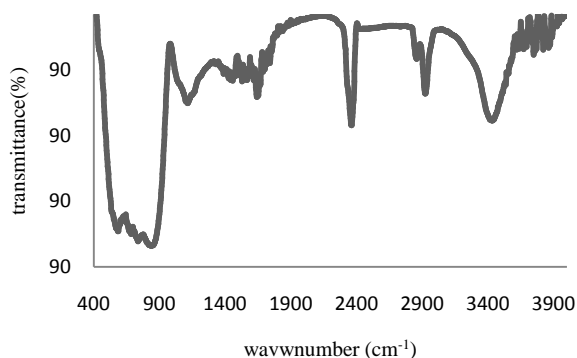

Fig.6. FTIR spectra of nano magnesium oxide.

Using reflection spectrum, $R(\omega)$, as function of wavenumber and Kramers-Kronig equation we can calculate phase change, $\varphi(\omega)$, and optical parameters[46, 47]. Reflection coefficient was obtained by following relations:

$$A = 2 - Ln(T\%) \qquad (2)$$

$$R = 100 - A - T \qquad (3)$$

Where A, T and R are absorption, transmittance and reflection, respectively. Using calculated $\varphi(\omega)$, refractive index and extinction coefficient calculated from[48]. The graphs of refractive index (n) and extinction coefficient (k) against wavenumber are given in Fig7.
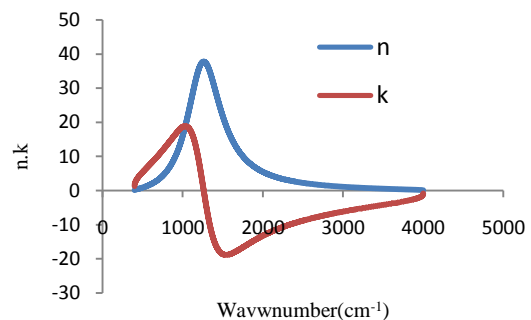

Fig.7. Refractive index (blue line) and extinction coefficient (red line) of nano MgO.

The refractive index values in this range of wavenumber are including two electron and ion contributions. Whatever the length of the wave goes smaller, light energy input increase and ionic contribution will decrease in the refractive index until the only remaining contribution is the electron. The refractive index reaches its maximum value with increasing wavenumber. Then it has a decreasing trend and desire to be a constant value. We can now calculate the real (ε') and imaginary (ε'') parts of the complex dielectric function ($\widetilde{\varepsilon}(\omega) = \varepsilon'(\omega) + i\varepsilon''(\omega)$) using $n(\omega)$ and $k(\omega)$ [49],

$$\qquad (4)$$

$$\qquad (5)$$

Then the real and imaginary parts of complex dielectric function versus wavenumber were plotted in Fig8.

$$\varepsilon'(\omega) = n^2(\omega) - k^2(\omega)$$

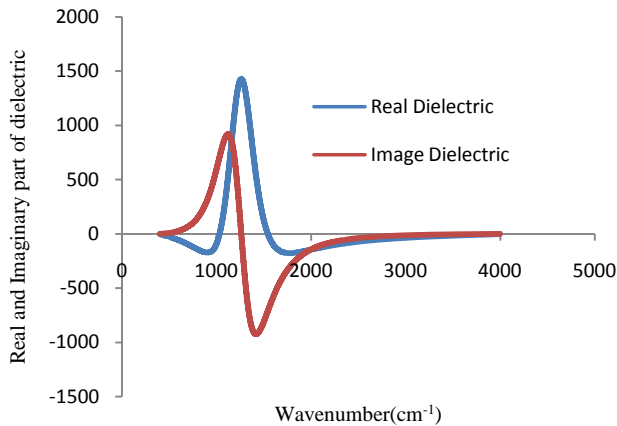$$\varepsilon''(\omega) = 2n(\omega)k(\omega)$$

Fig.8. Real and Imaginary part of dielectric for nano MgO.

We use this method to obtain longitudinal optical (LO) mode and transverse optical (TO) for MgO nano-powder. The dielectric function in the frequency between TO and LO is negative, in this area the wave doesn't propagate in the matter, and therefore, we expect that the reflection coefficient is large in this area. From the real part of the dielectric function graph can be set to LO and TO as a wavenumber, these values are 2117cm^{-1} and 1230cm^{-1}, respectively. Energy loss function, which defines the imaginary part of ε^{-1}, can be determined according to the following equations.

$$\frac{1}{\varepsilon} = \frac{\varepsilon' - i\varepsilon''}{(\varepsilon')^2 + (\varepsilon'')^2} \qquad (6)$$

$$-\mathrm{Im}\{\varepsilon^{-1}\} = \frac{\varepsilon''}{(\varepsilon')^2 - (\varepsilon'')^2} = \frac{2nk}{(n^2 + k^2)^2} \qquad (7)$$

The spectrum of energy loss function shows loss of energy particles that transmit through a solid. Energy loss function versus wavenumber in nano-powder is shown in Fig9.
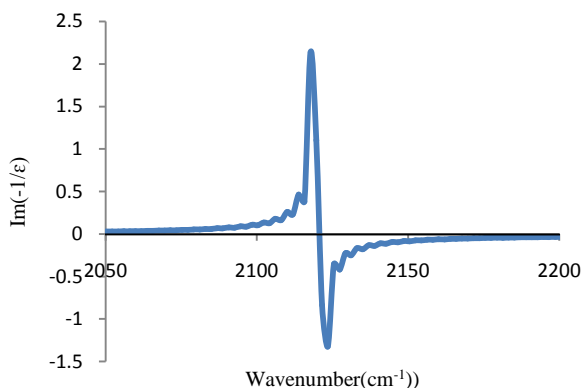

Fig.9. The spectrum of Im(-1/ε) for nano MgO

Imaginary part represents the energy loss in dielectric medium. As can be seen the maximum amount of Im(-1/ε) is at the wavenumber of 2118 cm^{-1} . In this wavenumber the most part of the incident light loss and therefore the application of nano MgO is not recommended in this wavenumber.

IV. CONCLUSION

Nano magnesium oxide synthesized by auto combustion method was characterized using XRD, TEM, UV-vis and FTIR and results was obtained as follows:

According to XRD, periclase is a main phase. Particle size is in the range of 30-80nm and the shape is nearly spherical to cubic. Uv-vis shows strong absorption at UV region at 285nm.Using UV-VIS band gap was calculated as 4.11ev. Regarding FTIR results and using kramers-kronig equation some optical parameters such as refractive index, extinction coefficient, real and imaginary dielectric and imaginary loss function achieved. The values of LO and TO was obtained 2117 cm^{-1} and 1230 cm^{-1} respectively.

ACKNOWLEDGMENT

REFERENCES

1. Xu, B. Q., Wei, J. M., Wang, H. Y., Sun, K. Q., & Zhu, Q. M, Nano-MgO: novel preparation and application as support of Ni catalyst for CO $_2$ reforming of methane. Catalysis Today, 2001. 68(1): p. 217-225.
2. Reddy, M. M., Ashoka, S., Chandrappa, G. T., & Pasha, M. A, Nano-MgO: an efficient catalyst for the synthesis of formamides from amines and formic acid under MWI. Catalysis letters, 2010. 138(1-2): p. 82-87.
3. Koo, K. Y., Roh, H. S., Seo, Y. T., Seo, D. J., Yoon, W. L., & Bin Park, S, A highly effective and stable nano-sized Ni/MgO–Al $_2$ O $_3$ catalyst for gas to liquids (GTL) process. International Journal of Hydrogen Energy, 2008. 33(8): p. 2036-2043.
4. Rakmak, N., Wiyaratn, W., Bunyakan, C., & Chungsiriporn, J, Synthesis of Fe/MgO nano-crystal catalysts by sol–gel method for hydrogen sulfide removal. Chemical Engineering Journal, 2010. 162(1): p. 84-90.
5. Shukla, S. K., Parashar, G. K., Mishra, A. P., Misra, P., Yadav, B. C., Shukla, R. K., ... & Dubey, G. C, Nano-like magnesium oxide films and its significance in optical fiber humidity sensor. Sensors and Actuators B: Chemical, 2004. 98(1): p. 5-11.
6. Karimi.M, A.L.I, Haghdar.R, S.A.E, I.D.Asadinia, R, Hatefi.M, A.A, Mashhadizadeh.M.H, Behjatmanesh.A.R, Zebarjad.S.M, Synthesis and characterization of nanoparticles and nano composite of ZnO and MgO by sonochemical method and their application for zinc polycarboxylate dental cement preparation. International nano letters(INL), 2011.
7. Nagappa, B. and G. Chandrappa, Mesoporous nanocrystalline magnesium oxide for environmental remediation. Microporous and Mesoporous Materials, 2007. 106(1): p. 212-218.
8. Huang, L., Li, D. Q., Lin, Y. J., Wei, M., Evans, D. G., & Duan, X, Controllable preparation of Nano-MgO and investigation of its bactericidal properties. Journal of inorganic biochemistry, 2005. 99(5): p. 986-993.
9. Kumar, A. and J. Kumar, On the synthesis and optical absorption studies of nano-size magnesium oxide powder. Journal of Physics and Chemistry of Solids, 2008. 69(11): p. 2764-2772.
10. Moon, H.R., J.J. Urban, and D.J. Milliron, Size-Controlled Synthesis and Optical Properties of Monodisperse Colloidal Magnesium Oxide Nanocrystals. Angewandte Chemie International Edition, 2009. 48(34): p. 6278-6281.

11. Jiu, J., Kurumada, K. I., Tanigaki, M., Adachi, M., & Yoshikawa, S, Preparation of nanoporous MgO using gel as structure-direct template. Materials Letters, 2004. 58(1): p. 44-47.

12. Chadwick, A. V., Poplett, I. J., Maitland, D. T., & Smith, M. E, Oxygen speciation in nanophase MgO from solid-state 17O NMR. Chemistry of materials, 1998. 10(3): p. 864-870.

13. Bokhimi, X., Morales, A., Portilla, M., & García-Ruiz, A, Hydroxides as precursors of nanocrystalline oxides. Nanostructured Materials, 1999. 12(1): p. 589-592.

14. Subramania, A., Kumar, G. V., Priya, A. S., & Vasudevan, T, Polyol-mediated thermolysis process for the synthesis of MgO nanoparticles and nanowires. Nanotechnology, 2007. 18(22): p. 225601.

15. López, T., Gómez, R., Navarrete, J., & López-Salinas, E, Evidence for Lewis and Brønsted Acid Sites on MgO Obtained by Sol-Gel. Journal of sol-gel science and technology, 1998. 13(1-3): p. 1043-1047.

16. Utamapanya, S., K.J. Klabunde, and J.R. Schlup, Nanoscale metal oxide particles/clusters as chemical reagents. Synthesis and properties of ultrahigh surface area magnesium hydroxide and magnesium oxide. Chemistry of materials, 1991. 3(1): p. 175-181.

17. Kim, J.Y., H.S. Jung, and K.S. Hong, Effects of Acetic Acid on the Crystallization Temperature of Sol–Gel-Derived MgO Nano-Powders and Thin Films. Journal of the American Ceramic Society, 2005. 88(3): p. 784-787.

18. Wang, J. A., Novaro, O., Bokhimi, X., Lopez, T., Gomez, R., Navarrete, J., ... & Lopez-Salinas, E, Characterizations of the thermal decomposition of brucite prepared by sol–gel technique for synthesis of nanocrystalline MgO. Materials Letters, 1998. 35(5): p. 317-323.

19. Wang, J. A., Bokhimi, X., Novaro, O., Lopez, T., & Gomez, R, Effects of the surface structure and experimental parameters on the isopropanol decomposition catalyzed with sol–gel MgO. Journal of Molecular Catalysis A: Chemical, 1999. 145(1): p. 291-300.

20. El-Shall, M. S., Slack, W., Vann, W., Kane, D., & Hanley, D, Synthesis of nanoscale metal oxide particles using laser vaporization/condensation in a diffusion cloud chamber. The Journal of Physical Chemistry, 1994. 98(12): p. 3067-3070.

21. Ding, Y., Zhang, G., Wu, H., Hai, B., Wang, L., & Qian, Y, Nanoscale magnesium hydroxide and magnesium oxide powders: control over size, shape, and structure via hydrothermal synthesis. Chemistry of materials, 2001. 13(2): p. 435-440.

22. Matthews, J. S., Just, O., Obi-Johnson, B., & Rees, W. S, CVD of MgO from a Mg (β-ketoiminate) 2: Preparation, Characterization, and Utilization of an Intramolecularly Stabilized, Highly Volatile, Thermally Robust Precursor. Chemical Vapor Deposition, 2000. 6(3): p. 129-132.

23. Helble, J.J., Combustion aerosol synthesis of nanoscale ceramic powders. Journal of aerosol science, 1998. 29(5): p. 721-736.

24. Bhargava, A., Alarco, J. A., Mackinnon, I. D., Page, D., & Ilyushechkin, A, Synthesis and characterisation of nanoscale magnesium oxide powders and their application in thick films of Bi$_2$Sr$_2$CaCu$_2$O$_8$. Materials Letters, 1998. 34(3): p. 133-142.

25. De Falco, G., Morgan, A., Commodo, M., Minutolo, P., & D'Anna, A, Flame synthesis of MgO nanoparticles in a FASP Reactor. MRS Online Proceedings Library, 2013. 1506: p. mrsf12-1506-y03-15.

26. McKenna, K. P., Koller, D., Sternig, A., Siedl, N., Govind, N., Sushko, P. V., & Diwald, O, Optical Properties of Nanocrystal Interfaces in Compressed MgO Nanopowders. ACS nano, 2011. 5(4): p. 3003-3009.

27. Aruna, S.T. and A.S. Mukasyan, Combustion synthesis and nanomaterials. Current Opinion in Solid State and Materials Science, 2008. 12(3): p. 44-50.

28. Fang, Y., Agrawal, D., Skandan, G., & Jain, M, Fabrication of translucent MgO ceramics using nanopowders. Materials Letters, 2004. 58(5): p. 551-554.

29. Athar, T., A. Hakeem, and W. Ahmed, Synthesis of MgO Nanopowder via Non Aqueous SolGel Method. Advanced Science Letters, 2012. 7(1): p. 27-29.

30. Mageshwari, K. and R. Sathyamoorthy, PREPARATION AND CHARACTERIZATION OF MgO NANOFLAKES BY WET PRECIPITATION METHOD.

31. Benedetti, S., Benia, H. M., Nilius, N., Valeri, S., & Freund, H. J, Morphology and optical properties of MgO thin films on Mo (001). Chemical physics letters, 2006. 430(4): p. 330-335.

32. Ricci, D., Bongiorno, A., Pacchioni, G., & Landman, U, Bonding trends and dimensionality crossover of gold nanoclusters on metal-supported MgO thin films. Physical review letters, 2006. 97(3): p. 036106.

33. Jung, H. S., Lee, J. K., Young Kim, J., & Hong, K. S, Synthesis of nano-sized MgO particle and thin film from diethanolamine-stabilized magnesium-methoxide. Journal of Solid State Chemistry, 2003. 175(2): p. 278-283.

34. Abbet, S., Heiz, U., Maria Ferrari, A., Giordano, L., Di Valentin, C., & Pacchioni, G, Nano-assembled Pd catalysts on MgO thin films. Thin solid films, 2001. 400(1): p. 37-42.

35. Kim, S.G., J.Y. Kim, and H.J. Kim, Deposition of MgO thin films by modified electrostatic spray pyrolysis method. Thin solid films, 2000. 376(1): p. 110-114.

36. Sterrer, M., Heyde, M., Novicki, M., Nilius, N., Risse, T., Rust, H. P., ... & Freund, H. J, Identification of color centers on MgO (001) thin films with scanning tunneling microscopy. The Journal of Physical Chemistry B, 2006. 110(1): p. 46-49.

37. Fu, X., Song, Z., Wu, G., Huang, J., Duo, X., & Lin, C, Preparation and characterization of MgO thin films by a novel sol-gel method. Journal of sol-gel science and technology, 1999. 16(3): p. 277-281.

38. Kaviyarasu, K. and P.A. Devarajan, A versatile route to synthesize MgO nanocrystals by combustion technique. Der Pharma Chemica, 2011. 3(5).

39. Bai, J. I. A. H. A. I., Meng, F. A. N. T. A. O., Wei, C. H. U. N. C. H. E. N. G., Zhao, Y., Tan, H., & Liu, J. U. N. C. H. E. N. G, Solution Combustion Synthesis and Characteristics of Nanoscale MgO Powders. Ceramics-Silikaty, 2011. 55(1): p. 20-25.

40. Stankic, S., Müller, M., Diwald, O., Sterrer, M., Knözinger, E., & Bernardi, J, Size-Dependent Optical Properties of MgO Nanocubes. Angewandte Chemie International Edition, 2005. 44(31): p. 4917-4920.

41. Prathap, P., Subbaiah, Y. V., Devika, M., & Reddy, K. T, Optical properties of In$_2$O$_3$ films prepared by spray pyrolysis. Materials chemistry and physics, 2006. 100(2): p. 375-379.

42. Bube, R., Electronic properties of crystalline solids: an introduction to fundamentals2012: Elsevier.

43. Taurian, O., M. Springborg, and N. Christensen, Self-consistent electronic structures of MgO and SrO. Solid state communications, 1985. 55(4): p. 351-355.

44. Ghasemifard, M., S. Hosseini, and G.H. Khorrami, Synthesis and structure of PMN–PT ceramic nanopowder free from pyrochlore phase. Ceramics International, 2009. 35(7): p. 2899-2905.

45. Selvam, N., Kumar, R. T., Kennedy, L. J., & Vijaya, J. J, Comparative study of microwave and conventional methods for the preparation and optical properties of novel MgO-micro and nano-structures. Journal of Alloys and Compounds, 2011. 509(41): p. 9809-9815.

46. Graf, R., J. Koenig, and H. Ishida, Optical constant determination of thin polymer films in the infrared. Applied spectroscopy, 1985. 39(3): p. 405-408.

47. Anicete-Santos, M., Silva, M. S., Orhan, E., Góes, M. S., Zaghete, M. A., Paiva-Santos, C. O., ... & Longo, E, Contribution of structural order–disorder to the room-temperature photoluminescence of lead zirconate titanate powders. Journal of Luminescence, 2007. 127(2): p. 689-695.

48. Shakeri-Zadeh, A., M. Ghasemifard, and G. Ali Mansoori, Structural and optical characterization of folate-conjugated gold-nanoparticles. Physica E: Low-dimensional Systems and Nanostructures, 2010. 42(5): p. 1272-1280.

49. Manifacier, J., J. Gasiot, and J. Fillard, A simple method for the determination of the optical constants n, k and the thickness of a weakly absorbing thin film. Journal of Physics E: Scientific Instruments, 1976. 9(11): p. 1002.